The Journal of Pathology, ORIGINAL PAPER

Upregulated expression and function of the α4β1 integrin in multiple myeloma cells resistant to bortezomib

Silvia Sevilla-Movilla[1], Nohemí Arellano-Sánchez[1], Mónica Martínez-Moreno[1], Consuelo Gajate[1], Anna Sánchez-Vencells[1], Luis Vitores Valcárcel[2], Xabier Agirre[2], Antonio Valeri[3], Joaquin Martínez-López[3], Felipe Prósper[2,4], Faustino Mollinedo[1] and Joaquin Teixidó[1]*

[1]Department of Molecular Biomedicine, Centro de Investigaciones Biológicas Margarita Salas (CSIC), 28040 Madrid, Spain;

[2]Centro de Investigación Médica Aplicada, Universidad de Navarra, 31008 Pamplona, Spain;

[3]Departament of Translational Hematology, Hospital Universitario 12 de Octubre, Centro Nacional de Investigaciones Oncológicas, CIBERONC, 28041 Madrid, Spain

[4]Departament of Hematology, Clínica Universidad de Navarra, Universidad de Navarra, 31009 Pamplona, Spain.

***Correspondence to:** J Teixidó. Centro de Investigaciones Biológicas Margarita Salas, Department of Molecular Biomedicine. Ramiro de Maeztu 9, 28040 Madrid, Spain. E-mail: joaquint@cib.csic.es

Running head: Myeloma resistance to bortezomib and α4β1 expression and function

This article has been accepted for publication and undergone full peer review but has not been through the copyediting, typesetting, pagination and proofreading process which may lead to differences between this version and the Version of Record. Please cite this article as doi:10.1002/path.5480

The authors declare no financial interests.

Word count 3988

ABSTRACT

The interaction of multiple myeloma (MM) cells with the bone marrow (BM) microenvironment promotes MM cell retention, survival and resistance to different anti-MM agents, including proteasome inhibitors (PIs) such as bortezomib (BTZ). The α4β1 integrin is a main adhesion receptor mediating MM cell-stroma interactions and MM cell survival, and its expression and function are downregulated by BTZ, leading to inhibition of cell adhesion-mediated drug resistance (CAM-DR) and MM cell apoptosis. Whether decreased α4β1 expression and activity is maintained or recovered upon development of resistance to BTZ represents an important question, as a potential rescue of α4β1 function could boost MM cell survival and disease progression. Using BTZ-resistant MM cells, we found that they not only rescue their α4β1 expression, but its levels were higher than in parental cells. Increased α4β1 expression in resistant cells correlated with enhanced α4β1-mediated cell lodging in the BM, and with disease progression. BTZ-resistant MM cells displayed enhanced NF-κB pathway activation relative to parental counterparts, which contributed to upregulated α4 expression and to α4β1-dependent MM cell adhesion. These data emphasize the upregulation of α4β1 expression and function as a key event during resistance to BTZ in MM, which might indirectly contribute to stabilize this resistance, as stronger MM cell attachment to BM stroma will regain CAM-DR and MM cell growth and survival. Finally, we found a strong correlation between high *ITGB1* (integrin β1) expression in MM and poor progression-free survival (PFS) and overall survival (OS) during treatment of MM patients with BTZ and IMIDs, and combination of high *ITGB1* levels and presence of the high-risk genetic factor amp1q causes low PFS and OS. These results unravel a novel prognostic value for *ITGB1* in myeloma.

Keywords: Multiple myeloma, Integrins, Proteasome inhibitors, Resistance, Prognosis

INTRODUCTION

Multiple myeloma is a hematological neoplasia characterized by clonal expansion of antibody-producing malignant plasma cells in the bone marrow (BM), causing osteolytic bone lesions, hypercalcemia, anemia and renal failure [1-5]. In spite that different treatments against MM including autologous stem cell transplantation, proteasome inhibitors, immunomodulatory drugs, chimeric antigen receptor (CAR) T cell and monoclonal antibody therapies have improved patient survival [6–10], the disease remains largely incurable.

The communication of MM cells with their surrounding BM microenvironment depends on specific adhesion receptor-ligand interactions, and is critical for MM cell localization and retention, for survival, and for resistance to chemotherapy [1,4]. MM cell trafficking to and inside the BM is based on the activity of the α4β1 (also called VLA-4) integrin [11–13]. A functional partner of α4β1 is CXCL12, an abundant chemokine in the BM, which upon binding to its receptor CXCR4 delivers stimulating signals for upregulation of α4β1-mediated MM cell adhesion [14–16]. The attachment of MM cells mediated by α4β1 to its ligands VCAM-1 and fibronectin, both present in the myeloma BM compartment, does not only provide MM cell localization, but it also contributes to cell survival and to cell adhesion-mediated drug resistance (CAM-DR). Thus, early studies revealed that α4β1-dependent MM cell adhesion to BM stromal cells induces IL-6 secretion, a key cytokine for MM cell proliferation and survival, and *in vivo* approaches demonstrated the importance of α4β1-mediated MM cell attachment for disease progression [17–19]. Furthermore, the humanized anti-α4 monoclonal antibody natalizumab was shown to decrease MM cell growth in the BM microenvironment [20]. The relevance of

α4β1 in promoting CAM-DR has been revealed in MM cells exposed to melphalan, doxorubicin, bortezomib (BTZ) and simvastin [21–23].

Proteasome inhibitors (PIs) represent common agents used against MM [6,24,25]. All approved PIs target the PSMβ5 subunit of the proteasome, including BTZ, carfilzomib (CFZ) and ixazomib [25]. Mutations in this subunit causing failure of BTZ binding to the proteasome represent a potential mechanism of MM cell resistance to this inhibitor [26-29]. Other reported mechanisms of resistance to PIs include clearance of misfolded proteins by autophagic elimination of aggresomes, aberrant NF-κB pathway activation, metabolic dysregulation, and involvement of the BM microenvironment [25,28]. Therefore, there is no a single primary mechanism absolutely responsible for providing resistance to PI in MM cells, which is an important clinical problem. Moreover, resistance to PIs might involve indirect cell responses directly impinging on primary resistance mechanisms.

BTZ can overcome CAM-DR by downregulating α4β1 expression in MM cells [23]. Similarly, a modulation by BTZ of the α4β1/VCAM-1 interaction involving hematopoietic stem and progenitor cell adhesion to the BM microenvironment was also reported [30]. Given the key role of α4β1 in MM disease progression, its downregulation in BTZ-exposed MM cells could affect their BM trafficking, retention and survival. However, whether the decreased α4β1 expression and function is maintained or recovered upon development of resistance to BTZ represents an important question which has not been addressed. A potential rescue of α4β1 expression and function could clearly affect the outcome of the disease. Here we have generated BTZ-resistant MM cells to uncover potential relationships between α4β1 expression and function and resistance to BTZ. Our data provide *in vitro* and *in vivo* evidence of rescue of high

α4β1 expression and activity in BTZ-resistant MM cells, highlighting a potential α4β1 role as indirect contributor of resistance to PIs. In addition, we have unveiled a prognostic value for *ITGB1* (integrin β1) expression combined with genetic biomarkers during MM treatment with therapies that include BTZ.

MATERIALS AND METHODS

Details for Cells, reagents and antibodies used, Flow cytometry, apoptosis and VCAM-1 binding assays, RNA interference, transfections and RT-qPCR are presented in Supplementary material, Supplementary materials and methods.

Cell proliferation and adhesion assays. A tetrazolium salt was used to estimate cell proliferation, according to manufacturer's instructions (CCK-8 kit, Sigma-Aldrich, St. Louis, MO, USA). In brief, cells were tested in triplicated, and after 2 h at 37 °C with CCK-8 solution, sample Absorbance was read at 450 nm (Multiskan Bichromatic, Labsystems, Vantaa, Finland). Assays of adhesion to α4β1 ligands were carried out as we described previously [31]. In brief, BCECF-AM-labeled cells were plated in triplicate in wells coated with the fibronectin recombinant fragment FN-H89 (CS-1/FN), that contains the α4β1-binding CS-1 region, or with recombinant VCAM-1, in the absence or presence of immobilized CXCL12. Plates were incubated for 2 min at 37 °C after a brief centrifugation (2 s, 1,200 rpm), and adhesion quantified using a fluorescence analyzer. Adhesion data is presented relative to control cells, which were given an arbitrary value of 100.

Immunoblotting. Cells were solubilized in lysis buffer (1% Nonidet P-40, 50 mM Tris-HCl pH 7.4, 100 mM NaCl, 2 mM $MgCl_2$, 10% glycerol) in the presence of protease and phosphatase inhibitors (Sigma Aldrich). Proteins were resolved by SDS-PAGE, transferred to PVDF membranes (Bio-Rad Laboratories, Hercules, CA, USA) and incubated with primary antibodies and horseradish peroxidase-conjugated secondary antibodies listed in supplementary material,

Table S2. Proteins were visualized using Immobilon Western (Millipore, Billerica, MA, USA) and a chemiluminescence detector (Fujifilm LAS 3000 Image Reader, Fujifilm, Tokyo, Japan).

***In vivo* studies.** The Consejo Superior de Investigaciones Científicas Ethics Committee approved the protocols used for experiments with mice. NOD/SCID/IL2gR$^{-/-}$ (NSG) mice were subcutaneously inoculated with 1.5×10^6 parental or BTZ-resistant NCI-H929 cells. When tumors were visually detected (around day 6), mice were randomly divided into two groups and intraperitoneally (i.p.) injected every 2 or 3 days with BTZ (0.8 mg/kg in PBS) or vehicle (DMSO in PBS), and tumor growth was monitored daily. RPMI-8226 and RPMI-8226-R7 cells were pre-incubated for 20 min at 37 °C with control (P3) or anti-α4 (ALC 1.63) antibodies (50 µg/ml) before inoculation into NSG mice (n=7-–9 per cell type). Cells ($3x10^6$) from the different groups were intravenously injected into the tail vein and were treated i.p. every 2-3 days with control or anti-α4 (300 µg/kg) antibodies. After approximately 4 weeks, mice injected with RPMI-8226-R7 cells and receiving control antibodies displayed hind limb paralysis, and then mice from all groups were sacrificed. MM cell infiltration in the BM of femurs was evaluated by flow cytometry (FACS) for expression of human HLA-1, and by RT-qPCR to determine human *GAPDH* versus mouse *Tbp* expression.

Survival studies. For survival analyses, we used the survival data from the IA14 release of the Multiple Myeloma Research Foundation (MMRF) CoMMpass Study dataset. In the progression-free survival (PFS) and overall survival (OS), we included 285 MM patients treated with bortezomib and immunomudulatory drugs (IMIDs). CoMMpass RNA-seq samples were processed with Salmon v0.9.1 using Gencode v27. We used the *maxStat* package (R) to select a

threshold value for the expression of the *ITGA4*, *ITGB1* and *CXCR4* genes. In order to avoid the bias introduced by this package, the threshold was selected as the median of 50,000 possible thresholds calculated with one third of the samples, randomly but balanced-selected. Using the threshold, we discretized the genes as lowly or highly expressed, and then performed univariate COX regressions. We searched the synergy with biomarkers published in IA14, selected and filtered using *LogRank* single variable regression performing a Monte Carlo simulation provided by *maxStat*, selecting only those variables with significant p-value. These variables were included in a multivariate cox regression in order to select the ones that remained significant.

Statistical analysis. Analyses were performed with GraphPad Prism 5. Outliers according to Grubbs' test were excluded. Two groups of normally-distributed data were compared using paired or unpaired *t*-tests. Results were considered significantly different when $p<0.05$. Values at $^{*}p<0.05$, $^{**}p< 0.01$, and $^{***}p<0.001$, denoted a significant decrease, whereas $^{\Delta}p<0.05$, $^{\Delta\Delta}p< 0.01$, and $^{\Delta\Delta\Delta}p<0.001$ indicated a significant increase.

RESULTS

Characterization of bortezomib-resistant myeloma cells. Two independent NCI-H929 myeloma cell cultures were exposed to gradual increases of BTZ concentrations, from 5 nM to 20 nM. When cells were with 20 nM BTZ in normal culture medium, cultures displayed a short quiescent period without apparent growth, which was surpassed by increasing FBS to 20% and adding IL-6. Once cells were back to normal proliferation rates, serum was decreased to 10% and IL-6 removed without affecting growth. Cell proliferation assays revealed that, compared to the strong growth inhibition of parental cells treated with BTZ, the two BTZ-resistant cell cultures, NCI-H929-R20.1 and NCI-H929-R20.2 display growth rates in the presence of BTZ similar to parental ones, although the R20.2 cells showed a slower rate (Figure 1A). We also obtained NCI-H929 cells continuously growing in BTZ 35 nM (NCI-H929-R35; see supplementary material, Figure S1A, left), although their proliferation was slower than that of R20 cells, what led us to use the later for the subsequent studies. NCI-H929-R20.1 cells not only proliferated in the presence of BTZ, but they were also resistant to carfilzomib (CFZ) (Figure 1B), suggesting that they might present general resistance to PIs. Growth inhibition of NCI-H929 cells by BTZ or CFZ was associated with apoptosis, while NCI-H929-R20.1 and NCI-H929-R35 cells incubated with these PIs exhibited no significant increase in apoptosis relative to non-treated cells (Figure 1C; see supplementary material, Figure S1A, right). NCI-H929-R20.1 cell resistance to BTZ was next tested *in vivo* in NSG mice. When subcutaneous tumors were evident, we treated mice with BTZ or vehicle, and periodically measured tumor volumes. Data revealed that NCI-H929-R20 cells generated faster and larger tumors than parental counterparts in vehicle-treated mice (Figure 1D). Whereas BTZ significantly inhibited NCI-H929 tumor growth, NCI-H929-R20 tumors displayed similar volumes at the end of the

experiment independently of treatment with BTZ or vehicle. These *in vivo* results confirm the resistance to BTZ of NCI-H929-R20 cells.

Further characterization of NCI-H929-R20 cells revealed full sensitivity to the anti-MM drugs Aplidin (plitidepsin) (see supplementary material, Figure S1B) and doxorubicin (not shown). To determine if resistance could involve drug extrusion by the ABC-family P-glycoprotein (PgP), we first performed FACS to compare PgP expression on NCI-H929 and NCI-H929-R20 cells. The results revealed that neither parental nor resistant cells expressed PgP, as compared with PgP-transfected LoVo cells used as positive controls (see supplementary material, Figure S1C). Moreover, when we combined BTZ and the PgP inhibitor verapamil [32], there was only a minor reduction (10%) in cell viability relative to BTZ treatment alone (see supplementary material, Figure S1D), indicating that resistance to BTZ was mostly independent of PgP activity.

As expected, parental NCI-H929 cells exposed to BTZ displayed accumulation of ubiquitinated proteins, indicating that the PI was inhibiting the proteasome (Figure 1E). Incubation of NCI-H929-R20 cells with BTZ also caused accumulation of ubiquitinated proteins but to a lesser extent than parental cells. Mutations on the *PSMB5* subunit of the proteasome have been implicated in resistance to BTZ [26,27]. Sequencing *PSMB5* revealed no mutations on NCI-H929-R20 cells (not shown), but RT-qPCR analyses showed that these cells have higher *PSMB5* levels than parental counterparts (Figure 1F), similar to previous observations in BTZ-resistant cells [33].

Bortezomib-resistant MM cells display higher α4β1 expression and function than parental cells. Analyses by qPCR of BTZ-treated primary $CD138^+$ MM bone marrow cells revealed a

remarkable decrease in *ITGA4* and *ITGB1* expression (Figure 2A). We found that this reduced expression was independent of disease stage, type (IgG or IgA *kappa*), degree of BM plasma cell infiltration, and the age and sex of patients. Similar to $CD138^+$ cells, BTZ-exposed parental NCI-H929 cells displayed a strong reduction in cell membrane α4 and β1 expression, whereas CXCR4 and integrin α5 expression decreased only moderately (Figure 2B, left). Of note, NCI-H929-R20.1 and -R20.2 cells displayed membrane expression levels of α4, β1 and α5 that were significantly higher than those of parental cells (Figure 2B, left and right; see supplementary material, Figure S1E). Instead, CXCR4 expression remained mostly unaltered. Consistent with the higher cell membrane expression of α4β1 in NCI-H929-R20 cells, immunoblotting assays showed increased α4 and β1 levels in these cells relative to parental cells (Figure 2C; see supplementary material, Figure S1F), which correlated with enhanced *ITGA4* and *ITGB1* levels (Figure 2D). In spite of the unchanged CXCR4 membrane expression on NCI-H929-R20 cells, we found higher *CXCR4* levels in these resistant cells than in parental ones (Figure 2D). Although both NCI-H929-R20.1 and NCI-H929-R20.2 cells exhibited upregulation of α4β1 expression, as the R20.1 cells grew better in culture than the R20.2 counterparts, we selected the former to functionally characterize BTZ-resistant MM cells in α4β1-dependent adhesion assays. In close correlation with upregulated α4β1 expression on NCI-H929-R20 cells, they displayed increased adhesion to the α4β1 ligands VCAM-1 and CS-1/FN, both in the absence and presence of co-immobilized CXCL12 (Figure 2E). Moreover, soluble VCAM-1 binding was higher on the BTZ-resistant than on the parental cells (Figure 2F).

To determine if upregulation of α4β1 expression seen on NCI-H929-R20 cells could also be detected in other MM cell lines, we used the previously reported BTZ-resistant RPMI-8226-

R7 and RPMI-8226-R100 cells [27]. These cells display upregulation of mutant *PSMB5* proteasome subunit that affects BTZ binding, causing resistance to this inhibitor. In line with these observations, we found no accumulation of ubiquitinated proteins in BTZ-treated RPMI-8226-R7 and RPMI-8226-R100 cells compared to parental cells (see supplementary material, Figure S2A).

Analogous to the NCI-H929 parental-resistant cell pair, FACS experiments revealed that both RPMI-8226-R7 and RPMI-8226-R100 cells have higher α4β1 expression than parental cells (Figure 3A). Unlike NCI-H929-R20 cells, BTZ-resistant RPMI-8226 cells displayed enhanced CXCR4 membrane expression, whereas α5 integrin levels were reduced. Consistent with the FACS data, immunoblotting analyses showed that α4 and β1 expression was upregulated in resistant RPMI-8226 cells (Figure 3B). In addition, both RPMI-8226-R7 and RPMI-8226-R100 cells cultured for 3 weeks without the PI retained resistance to BTZ (see supplementary material, Figure S2B) and higher α4 and β1 levels than parental cells (Figure 3C), indicating that resistance and increased α4β1 expression were independent of the continuous cell exposure to BTZ.

The expression of *ITGA4* and *CXCR4* was significantly higher in BTZ-resistant RPMI-8226 than parental cells (Figure 3D), correlating with their enhanced protein levels, whereas *ITGB1* expression was elevated in RPMI-8226-R100 but not in RPMI-8226-R7 cells (Figure 3D). These results indicated that upregulated α4 expression in NCI-H929 and RPMI-8226 resistant cells is at least transcriptionally-based. To determine if increased β1 protein expression involved its stabilization, we treated RPMI-8226-R7 and RPMI-8226-R100 cells with cycloheximide and analyzed β1 levels by immunoblotting. The results revealed reduced β1

expression in cycloheximide-treated parental cells, whereas β1 accumulated in resistant cells exposed to cycloheximide (Figure 3E), indicating that increased β1 stability in resistant RPMI-8226 cells represents one of the mechanisms responsible for its upregulation.

Next, we tested BTZ-resistant RPMI-8226 cells in adhesion assays to α4β1 ligands co-immobilized with CXCL12, as they express elevated CXCR4 membrane levels. The results revealed significantly higher α4β1-mediated adhesion of RPMI-8226-R7 cells than parental counterparts (Figure 4A). Importantly, these resistant cells displayed a remarkable increase in lodging to the BM of NSG mice associated with hind limb paralysis relative to parental cells, as detected by specific human HLA-1^{+} expression. Notably, the upregulated resistant cell infiltration was blocked by anti-α4 antibodies, indicating the involvement of α4β1 in cell lodging in the BM (Figure 4B, left). Examination of the infiltrated MM cells from the BM indicated that resistant cells retained higher α4 expression than the parental cells (Figure 4B, right). Moreover, qPCR analyses of human *GAPDH* versus mouse *TBP* expression further supported the increased α4β1-dependent RPMI-8226-R7 cell lodging in the BM compared to parental cells (Figure 4C).

BTZ-resistant MCL and T-ALL cells do not display upregulated α4β1 expression and function. Mantle cell lymphoma (MCL) is another hematological malignancy which can be treated with BTZ [34]. We generated BTZ-resistant Z-138 cells (Z-138-R10; resistant to 10 nM BTZ), as a model for MCL (see supplementary material, Figure S3A) to look for potential changes in α4β1 expression. Contrary to BTZ-resistant MM cells, FACS and immunoblotting analyses revealed no increased α4, β1 and CXCR4 expression in Z-138-R10 cells relative to untreated parental ones (see supplementary material, Figures S3B, S3C). Consistently, we did

not find significant variations between α4β1-dependent Z-138 and Z-138-R10 cell adhesion levels (see supplementary material, Figure S3D). T cell acute lymphoblastic leukemia (T-ALL) cells have been also found to be sensitive to BTZ [35]. We obtained BTZ-resistant Molt-4 cells (Molt-4-R7; resistant to 7 nM BTZ) as a T-ALL model (see supplementary material, Figure S3E). These cells displayed downregulated α4 and CXCR4 expression relative to parental counterparts, whereas the cell membrane β1 levels were enhanced both in parental and Molt-4-R7 cells following BTZ treatment (see supplementary material, Figure S3F). Yet, no significant changes between α4β1-mediated parental and BTZ-resistant Molt-4 cell adhesion were detected (see supplementary material, Figure S3G). These results suggest that the enhanced α4β1 expression and function seen in BTZ-resistant MM cells cannot be generalized to MCL and T-ALL neoplasms.

Role of NF-κB in the upregulated α4β1 expression on BTZ-resistant MM cells. Aberrant activation of the NF-κB pathway is frequent during MM progression and in BTZ-resistant MM cells [36-41]. Phosphorylation of p65 NF-κB at Ser^{536} is associated with transcriptional activity [42-45]. BTZ treatment of NCI-H929 and RPMI-8226-R7 cells upregulated phosphorylation at Ser^{536} p65, and the increased phosphorylation remained higher in BTZ-resistant than in untreated parental cells (Figure 5A), revealing the activation of the canonical NF-κB pathway in the resistant cells. Correlating with NF-κB pathway activation, the expression of two NF-κB targets, *BIRC5* (also called Survivin) and *HIF1A* according to Hugo [46–49] was significantly enhanced in the resistant cells compared to parental ones (Figure 5B). Of note, interfering with NF-κB activation in NCI-H929-R20.1 cells with the IKK inhibitor BAY-11-7082 significantly downregulated the expression of *BIRC5,* and also reduced *ITGA4* levels, while *ITGB1*

expression was mostly unaltered (Figure 5C). Moreover, NF-κB1 silencing correlated with a significant decrease in *ITGA4* and α4 cell membrane levels (Figure 5D, 5E, left), further suggesting a NF-κB role in the regulation of α4 expression in the resistant cells. Reduced α4 surface expression correlated with a moderate decrease in NCI-H929-R20.1 cell attachment to CS-1/FN, although without reaching statistical significance (Figure 5E, right). These results suggest an involvement of NF-κB in the upregulated expression of α4β1 in BTZ-resistant MM cells.

Prognostic value of *ITGB1* in MM treatment with BTZ. To assess whether expression levels of *ITGA4*, *ITGB1* or *CXCR4* could correlate with the prognosis of MM patients exposed to therapies that include BTZ, we analyzed the progression-free survival (PFS) and overall survival (OS) of patients in the MMRF CoMMpass study during treatment with BTZ and IMIDs. These analyses were performed, according to the expression levels of each gene, and separating cases into two groups based on the distribution of expression levels. Whereas the expression levels of *ITGA4* and *CXCR4* at diagnosis did not correlate with prognosis, high *ITGB1* expression was significantly associated with lower PFS and OS in MM patients included in the BTZ-IMIDs treatment (Figure 6A,B). When a multivariate analysis was performed combining the expression of other known high-risk genetic factors, the combination of high *ITGB1* expression with amp1q resulted in statistically significant decrease in PFS and OS (Figure 6C,D). When these 2 prognostic factors were combined, MM patients could be stratified into four groups with significant differences in PFS and OS (Figure 6E,F). These results demonstrate that combination of *ITGB1* expression with established genetic biomarkers could have an important impact in prognosis of MM patients during the treatment with BTZ-IMIDs.

DISCUSSION

Natural and acquired resistance to PIs represents a serious clinical challenge in MM treatment [25,28]. The interaction of MM cells with their surrounding BM microenvironment provides CAM-DR to PIs as well as to other anti-MM agents [21,22]. The α4β1 integrin is a main adhesion receptor involved in MM cell-stroma interactions and MM cell survival [12,17,19,20], and plays key roles in CAM-DR [11-13].

Bortezomib downregulates the expression of α4β1 in MM cell lines, leading to inhibition of CAM-DR [22,23]. Likewise, we show here that BTZ treatment of $CD138^+$-selected BM cells from MM patients resulted in decreased *ITGA4* and *ITGB1* expression, and we confirm that this treatment reduces α4β1 myeloma cell membrane levels. Using BTZ-resistant NCI-H929 and RPMI-8226 cells, we found that they not only autonomously rescue their α4β1 expression upon development of resistance, but the integrin levels became higher than those of parental cells. Increased α4β1 expression had important functional consequences, as α4β1-mediated MM cell attachment to VCAM-1 and fibronectin was higher in resistant than in parental cells. Moreover, we show by two different parameters that BTZ-resistant RPMI-8226 cells have an increased α4β1-dependent capacity to lodge in the BM of NSG mice and to promote disease progression, as compared to parental cells. The enhanced BM lodging of the resistant cells mediated by α4β1 is likely contributed by their upregulated CXCR4 expression. Accordingly, the interaction between myeloma cell CXCR4 and CXCL12 present in the BM will likely increase α4β1 activity on resistant MM cells, facilitating their BM lodging. Of note, chemoresistant minimal residual disease (MRD) MM clones, including those resistant to BTZ, were enriched in cells overexpressing α4β1 relative to diagnostic clonal cells from MM patients

[50]. Together with our results, these data highlight the upregulation of α4β1 expression and function as an important and unwanted event which might indirectly contribute to chemoresistance to BTZ in MM. Thus, increased α4β1 expression could facilitate renewed and stronger MM cell attachment and retention by BM stroma, regaining the CAM-DR and favoring MM cell growth and survival. In addition, the data suggest that the enhanced α4β1 expression in BTZ-resistant MM cells could facilitate early identification of BTZ-treated patients developing resistance. Upregulated α4β1 levels were also reported in RPMI-8226 cells resistant to melphalan and doxorubicin [21], and increased expression of β1 integrin in BM cells from MM patients treated with melphalan-based regimens was found relative to pre-treatment [51], indicating that increased α4β1 expression might represent a common response during progression to resistance to different MM treatments.

We found that the increased expression of the α4 subunit in BTZ-resistant MM cells has at least a transcriptional basis, although we cannot rule out that post-transcriptional events could also facilitate the α4 upregulation. Likewise, the enhanced β1 expression has a clear transcriptional basis in NCI-H929-R20 cells, and a tendency in RPMI-8226-R7 cells. Data from cycloheximide-exposed BTZ-resistant RPMI-8226 cells revealed that increased β1 expression is facilitated by its higher stability, likely contributing to upregulated cell adhesion. Similar to previous data [37,41], we found higher activation of the NF-κB pathway in the BTZ-resistant MM cells than in the parental counterparts. Moreover, using both an inhibitor of IKK that inactivates NF-κB, and siRNA-mediated NF-κB silencing, we show that increased NF-κB pathway activation in NCI-H929-R20 cells contribute to the upregulated *ITGA4* expression, leading to increased α4 cell membrane levels. It is noteworthy that NF-κB depletion only

partially decreased α4 cell membrane expression, which correlated with a moderate reduction in α4β1-dependent MM cell adhesion, indicating that other unidentified factors are also involved in the upregulated α4 expression and function in BTZ-resistant MM cells. Unlike *ITGA4*, IKK inhibition did not alter *ITGB1* levels, suggesting that upregulation of *ITGB1* expression in NCI-H929-R20 cells is independent of NF-κB pathway activation.

Increased CXCR4 membrane expression was also observed in BTZ-resistant RPMI-8226 cells, but not on NCI-H929-R20 cells. Enhanced cell membrane CXCR4 levels have also been noted in myeloma MRD [50], although reduced CXCR4 expression was reported in mouse MM cells resistant to BTZ and in BTZ-treated MM patients [52]. Thus, further work is needed to unravel the cellular and molecular basis regulating CXCR4 expression in MM cells exposed to BTZ.

The molecular mechanisms accounting for resistance in NCI-H929-R20 cells have not been addressed in the present study. Mutations on *PSBM5* affecting BTZ binding proteasome, as well as overexpression of the β5 proteasome subunit were previously reported to mediate acquired resistance to BTZ in RPMI-8226 cells [26,27]. Although we did not detect mutations on *PSBM5* in NCI-H929-R20 cells, the reduced accumulation of ubiquitinated proteins in these cells relative to parental cells suggest some disfunction in their proteasomes, which might include decreased BTZ binding to proteasomes. Similar to the present data, previous studies showed no mutations on *PSBM5* in BTZ-resistant MM cells [53]. We did observe upregulated *PSBM5* expression in NCI-H929-R20 cells, which might contribute to BTZ resistance.

Finally, we found a significant correlation between high *ITGB1* expression in MM cells from patients at diagnosis and poor PFS and OS following treatment with BTZ and IMIDs.

Furthermore, combination of high *ITGB1* expression and presence of the high-risk genetic factor amp1q causes low PFS and OS, therefore unraveling a novel prognostic value for *ITGB1* in these MM patients and suggesting that high β1 expression might identify MM patients with high risk of disease progression.

ACKNOWLEDGMENTS

We thank Drs. Lisardo Boscá, Manuel Fresno and María Luisa Martín-Ramos for helpful suggestions, and Drs. Angeles García-Pardo, Alicia G. Arroyo, Patricia Boya, Giovanna Roncador, Luis F. García-Fernández and Carlos Galmarini for providing useful reagents. Dr. Pedro Lastres is acknowledged for help in flow cytometry, Francisco Casado-Robledillo and Olivia Barcón-Minchán for assistance in the Animal Facility, and Mireia Teixidó-Gironès for figure editing. We particularly acknowledge the patients for their participation, and the Biobank of the University of Navarra for its collaboration.

This work was supported by grants SAF2014-53059-R and SAF2017-85146-R from the Ministerio de Ciencia, Innovación y Universidades (MCIU) to JT; SAF2017-89672-R from MCIU to FM; by the Research Institute Hospital 12 de Octubre (i+12) and grants from Instituto de Salud Carlos III (ISCIII) and CIBERONC to JML; by grants from ISCIII PI16/02024, PI17/00701 and PI19/01352, TRASCAN (EPICA and Immunocell), Fundació La Marató de TV3, the Accelerator award CRUK/AIRC/AECC joint funder-partnership, CIBERONC (CB16/12/00489) and co-financed with FEDER funds MINECO Explora (RTHALMY), Gobierno de Navarra, Departamento de Salud 40/2016 and Departamento de Industria (Proyecto Estrategico, Reto Genomica, DIANA) and Fundación Ramón Areces (PREMAMM) to FP and XA The study was also supported by the Multiple Myeloma Research Foundation Networks of excellence, the International Myeloma Foundation (Brian van Novis), and the Qatar National Research Fund award 7-916-3-237.

Author contributions statement

SSM, MMM, CG, FM and JT conceived and carried out the experiments, and analyzed the data. NAS and ASV carried out experiments. LVV, XA and FP carried out the bioinformatics analyses. SSM, MMM, CG, XA, FP, FM, AV, JML and JT analyzed the results. All authors were involved in writing the paper and had final approval of the submitted and published versions.

REFERENCES

1. Hideshima T, Mitsiades C, Tonon G, *et al.* Understanding multiple myeloma pathogenesis in the bone marrow to identify new therapeutic targets. *Nat Rev Cancer* 2007; **7**: 585-598.
2. Kuehl WM, Bergsagel PL. Molecular pathogenesis of multiple myeloma and its premalignant precursor. *J Clin Invest* 2012; **122**: 3456-3463.
3. Morgan GJ, Walker BA, Davies FE. The genetic architecture of multiple myeloma. *Nat Rev Cancer* 2012; **12**: 335-348.
4. Bianchi G, Munshi NC. Pathogenesis beyond the cancer clone(s) in multiple myeloma. *Blood* 2015; **125**: 3049-3058.
5. van Nieuwenhuijzen N, Spaan I, Raymakers R, *et al.* From MGUS to Multiple Myeloma, a Paradigm for Clonal Evolution of Premalignant Cells. *Cancer Res* 2018; **78**: 2449-2456.
6. Orlowski RZ, Lonial S. Integration of novel agents into the care of patients with multiple myeloma. *Clin Cancer Res* 2016; **22**: 5443-5452.
7. Kumar SK, Anderson KC. Immune therapies in multiple myeloma. *Clin Cancer Res* 2016; **22**: 5453-5460.
8. Hoyos V, Borrello I. The immunotherapy era of myeloma: monoclonal antibodies, vaccines, and adoptive T-cell therapies. *Blood* 2016; **128**: 1679-1687.
9. Chim CS, Kumar SK, Orlowski RZ, *et al.* Management of relapsed and refractory multiple myeloma: novel agents, antibodies, immunotherapies and beyond. *Leukemia* 2018; **32**: 252-262.
10. Velasquez MP, Bonifant CL, Gottschalk S. Redirecting T cells to hematological malignancies with bispecific antibodies. *Blood* 2018; **131**: 30-38.
11. Ghobrial IM. Myeloma as a model for the process of metastasis: implications for therapy. *Blood* 2012; **120**: 20-30.
12. Martinez-Moreno M, Leiva M, Aguilera-Montilla N, *et al.* In vivo adhesion of malignant B cells to bone marrow microvasculature is regulated by alpha4beta1 cytoplasmic-binding proteins. *Leukemia* 2016; **30**: 861-872.
13. Redondo-Munoz J, Garcia-Pardo A, Teixido J. Molecular players in hematologic tumor cell trafficking. *Front Immunol* 2019; **10**: 156.
14. Sanz-Rodriguez F, Hidalgo A, Teixido J. Chemokine stromal cell-derived factor-1alpha modulates VLA-4 integrin-mediated multiple myeloma cell adhesion to CS-1/fibronectin and VCAM-1. *Blood* 2001; **97**: 346-351.
15. Alsayed Y, Ngo H, Runnels J, *et al.* Mechanisms of regulation of CXCR4/SDF-1 (CXCL12)-dependent migration and homing in multiple myeloma. *Blood* 2007; **109**: 2708-2717.
16. Azab AK, Runnels JM, Pitsillides C, *et al.* CXCR4 inhibitor AMD3100 disrupts the interaction of multiple myeloma cells with the bone marrow microenvironment and enhances their sensitivity to therapy. *Blood* 2009; **113**: 4341-4351.
17. Lokhorst HM, Lamme T, de Smet M, *et al.* Primary tumor cells of myeloma patients induce interleukin-6 secretion in long-term bone marrow cultures. *Blood* 1994; **84**: 2269-2277.

18. Mori Y, Shimizu N, Dallas M, *et al.* Anti-alpha4 integrin antibody suppresses the development of multiple myeloma and associated osteoclastic osteolysis. *Blood* 2004; **104**: 2149-2154.
19. Olson DL, Burkly LC, Leone DR, *et al.* Anti-alpha4 integrin monoclonal antibody inhibits multiple myeloma growth in a murine model. *Mol Cancer Ther* 2005; **4**: 91-99.
20. Podar K, Zimmerhackl A, Fulciniti M, *et al.* The selective adhesion molecule inhibitor Natalizumab decreases multiple myeloma cell growth in the bone marrow microenvironment: therapeutic implications. *Br J Haematol* 2011; **155**: 438-448.
21. Damiano JS, Cress AE, Hazlehurst LA, *et al.* Cell adhesion mediated drug resistance (CAM-DR): role of integrins and resistance to apoptosis in human myeloma cell lines. *Blood* 1999; **93**: 1658-1667.
22. Schmidmaier R, Baumann P, Simsek M, *et al.* The HMG-CoA reductase inhibitor simvastatin overcomes cell adhesion-mediated drug resistance in multiple myeloma by geranylgeranylation of Rho protein and activation of Rho kinase. *Blood* 2004; **104**: 1825-1832.
23. Noborio-Hatano K, Kikuchi J, Takatoku M, *et al.* Bortezomib overcomes cell-adhesion-mediated drug resistance through downregulation of VLA-4 expression in multiple myeloma. *Oncogene* 2009; **28**: 231-242.
24. Lub S, Maes K, Menu E, *et al.* Novel strategies to target the ubiquitin proteasome system in multiple myeloma. *Oncotarget* 2016; **7**: 6521-6537.
25. Gandolfi S, Laubach JP, Hideshima T, *et al.* The proteasome and proteasome inhibitors in multiple myeloma. *Cancer Metastasis Rev* 2017; **36**: 561-584.
26. Ri M, Iida S, Nakashima T, *et al.* Bortezomib-resistant myeloma cell lines: a role for mutated PSMB5 in preventing the accumulation of unfolded proteins and fatal ER stress. *Leukemia* 2010; **24**: 1506-1512.
27. Franke NE, Niewerth D, Assaraf YG, *et al.* Impaired bortezomib binding to mutant beta5 subunit of the proteasome is the underlying basis for bortezomib resistance in leukemia cells. *Leukemia* 2012; **26**: 757-768.
28. Wallington-Beddoe CT, Sobieraj-Teague M, Kuss BJ, *et al.* Resistance to proteasome inhibitors and other targeted therapies in myeloma. *Br J Haematol* 2018; **182**: 11-28.
29. Barrio S, Stuhmer T, Da-Via M, *et al.* Spectrum and functional validation of PSMB5 mutations in multiple myeloma. *Leukemia* 2019; **33**: 447-456.
30. Ghobadi A, Rettig MP, Cooper ML, *et al.* Bortezomib is a rapid mobilizer of hematopoietic stem cells in mice via modulation of the VCAM-1/VLA-4 axis. *Blood* 2014; **124**: 2752-2754.
31. Garcia-Bernal D, Redondo-Munoz J, Dios-Esponera A, *et al.* Sphingosine-1-phosphate activates chemokine-promoted myeloma cell adhesion and migration involving alpha4beta1 integrin function. *J Pathol* 2013; **229**: 36-48.
32. Gottesman MM, Pastan I. Biochemistry of multidrug resistance mediated by the multidrug transporter. *Annu Rev Biochem* 1993; **62**: 385-427.
33. Balsas P, Galan-Malo P, Marzo I, *et al.* Bortezomib resistance in a myeloma cell line is associated to PSMbeta5 overexpression and polyploidy. *Leuk Res* 2012; **36**: 212-218.
34. Robak T, Huang H, Jin J, *et al.* Bortezomib-based therapy for newly diagnosed mantle-cell lymphoma. *N Engl J Med* 2015; **372**: 944-953.

35. Koyama D, Kikuchi J, Hiraoka N, *et al.* Proteasome inhibitors exert cytotoxicity and increase chemosensitivity via transcriptional repression of Notch1 in T-cell acute lymphoblastic leukemia. *Leukemia* 2014; **28**: 1216-1226.
36. Annunziata CM, Davis RE, Demchenko Y, *et al.* Frequent engagement of the classical and alternative NF-kappaB pathways by diverse genetic abnormalities in multiple myeloma. *Cancer Cell* 2007; **12**: 115-130.
37. Hideshima T, Ikeda H, Chauhan D, *et al.* Bortezomib induces canonical nuclear factor-kappaB activation in multiple myeloma cells. *Blood* 2009; **114**: 1046-1052.
38. Demchenko YN, Glebov OK, Zingone A, *et al.* Classical and/or alternative NF-kappaB pathway activation in multiple myeloma. *Blood* 2010; **115**: 3541-3552.
39. Chapman MA, Lawrence MS, Keats JJ, *et al.* Initial genome sequencing and analysis of multiple myeloma. *Nature* 2011; **471**: 467-472.
40. Matthews GM, de Matos Simoes R, Dhimolea E, *et al.* NF-kappaB dysregulation in multiple myeloma. *Semin Cancer Biol* 2016; **39**: 68-76.
41. Markovina S, Callander NS, O'Connor SL, *et al.* Bortezomib-resistant nuclear factor-kappaB activity in multiple myeloma cells. *Mol Cancer Res* 2008; **6**: 1356-1364.
42. Sakurai H, Chiba H, Miyoshi H, *et al.* IkappaB kinases phosphorylate NF-kappaB p65 subunit on serine 536 in the transactivation domain. *J Biol Chem* 1999; **274**: 30353-30356.
43. O'Mahony AM, Montano M, Van Beneden K, *et al.* Human T-cell lymphotropic virus type 1 tax induction of biologically Active NF-kappaB requires IkappaB kinase-1-mediated phosphorylation of RelA/p65. *J Biol Chem* 2004; **279**: 18137-18145.
44. Yang F, Tang E, Guan K, *et al.* IKK beta plays an essential role in the phosphorylation of RelA/p65 on serine 536 induced by lipopolysaccharide. *J Immunol* 2003; **170**: 5630-5635.
45. Jiang X, Takahashi N, Matsui N, *et al.* The NF-kappa B activation in lymphotoxin beta receptor signaling depends on the phosphorylation of p65 at serine 536. *J Biol Chem* 2003; **278**: 919-926.
46. Shishodia S, Sethi G, Konopleva M, *et al.* A synthetic triterpenoid, CDDO-Me, inhibits IkappaBalpha kinase and enhances apoptosis induced by TNF and chemotherapeutic agents through down-regulation of expression of nuclear factor kappaB-regulated gene products in human leukemic cells. *Clin Cancer Res* 2006; **12**: 1828-1838.
47. Kawakami H, Tomita M, Matsuda T, *et al.* Transcriptional activation of survivin through the NF-kappaB pathway by human T-cell leukemia virus type I tax. *Int J Cancer* 2005; **115**: 967-974.
48. van Uden P, Kenneth NS, Rocha S. Regulation of hypoxia-inducible factor-1alpha by NF-kappaB. *Biochem J* 2008; **412**: 477-484.
49. van Uden P, Kenneth NS, Webster R, *et al.* Evolutionary conserved regulation of HIF-1beta by NF-kappaB. *PLoS Genet* 2011; **7**: e1001285.
50. Paiva B, Corchete LA, Vidriales MB, *et al.* Phenotypic and genomic analysis of multiple myeloma minimal residual disease tumor cells: a new model to understand chemoresistance. *Blood* 2016; **127**: 1896-1906.
51. Kurata M, Nakagawa Y, Yamamoto K, *et al.* Induction of integrin beta1 expression in bone marrow cells after chemotherapy correlates with the overexpression of lung

resistance protein and poor outcome in patients with multiple myeloma. *Am J Hematol* 2008; **83**: 755-757.
52. Stessman HA, Mansoor A, Zhan F, *et al.* Reduced CXCR4 expression is associated with extramedullary disease in a mouse model of myeloma and predicts poor survival in multiple myeloma patients treated with bortezomib. *Leukemia* 2013; **27**: 2075-2077.
53. Gutman D, Morales AA, Boise LH. Acquisition of a multidrug-resistant phenotype with a proteasome inhibitor in multiple myeloma. *Leukemia* 2009; **23**: 2181-2183.

FIGURE LEGENDS

Figure 1. Characterization of bortezomib-resistant NCI-H929 cells. Parental and BTZ-resistant cells were treated for the indicated times without or with BTZ (20 nM) (A), or for 48 h with CFZ (40 nM) (B), and subsequently subjected to proliferation assays with CCK8 (n=3 or 4). Proliferation was reduced $^{***}p<0.001$, or augmented $^{\Delta\Delta\Delta}p<0.001$). (C) Cells were incubated for 48 h with BTZ or CFZ (20 and 40 nM, respectively), and the apoptotic rates determined by flow cytometry (n=3). (D) Parental and BTZ-resistant NCI-H929 cells were subcutaneously inoculated into NSG mice, and when tumors started to grow, mice were treated with either DMSO (Ctrl) or BTZ in DMSO. Shown are tumor volumes at different time points (n=5-8; $^{*}p<0.05$). (E) Cells were treated for the indicated times without (-) or with BTZ (20 nM), and expression of ubiquitinated proteins was analyzed by immunoblotting. (F) Expression of PSMβ5 in parental and resistant cells was determined by RT-qPCR ($^{\Delta\Delta}p<0.01$).

Figure 2. Bortezomib-resistant NCI-H929 cells show higher α4β1 expression and function than parental cells. (A) $CD138^{+}$ primary BM myeloma cells incubated for 48 h without (-) or with (+) BTZ (20 nM) were tested by RT-qPCR to determine *ITGA4* and *ITGB1* expression (n=3-4; $^{*}p<0.05$). (B, left) Parental and BTZ-resistant NCI-H929 cells were incubated as in (A), and subsequently subjected to flow cytometry for detection of the indicated surface markers. Data show fold-induction of fluorescence intensity values referred to parental cells that were given a value of 100 (n=5; $^{\Delta}p<0.05$). (Right) Shown are representative histograms for α4 and β1 expression in parental and resistant cells. (C) Cells were treated with or without BTZ (20 nM) and analyzed by immunoblotting to test for α4 and β1 expression. (D) Cells were analyzed by

RT-qPCR to determine *ITGA4*, *ITGB1* and *CXCR4* expression (n=4; $^{\Delta\Delta}p<0.01$, $^{\Delta}p<0.05$). (E) Cells were subjected to adhesion assays to the indicated α4β1 ligands coimmobilized without (Medium) or with CXCL12 (n=3-4; $^{\Delta\Delta}p<0.01$, $^{\Delta}p<0.05$). (F) Cells were incubated in the absence or presence of CXCL12, and the binding of VCAM-1-Fc was determined by flow cytometry (n=3; $^{\Delta\Delta\Delta}p<0.001$, $^{\Delta\Delta}p<0.01$).

Figure 3. Bortezomib-resistant RPMI-8226 myeloma cells show higher α4β1 expression than parental cells. (A, left) Cells were incubated for 48 h without (-) or with (+) BTZ (7 or 100 nM), and afterwards subjected to flow cytometry for detection of the indicated markers. Data display fold induction of fluorescence intensity values relative to parental cells that were given a value of 100 (n=5; $^{\Delta\Delta\Delta}p<0.001$, $^{\Delta\Delta}p<0.01$ and $^{\Delta}p<0.05$). (Right) Shown are representative histograms for α4 and β1 expression in parental and resistant cells. (B) Cells were treated with or without BTZ and analyzed by immunoblotting for α4 and β1 expression. (C) Cells were cultured for 3 weeks in the absence (-) or presence (+) of BTZ (7 or 100 nM), and subsequently treated with or without the inhibitor and the α4 and β1 expression was analyzed by western blotting. (D) Cells were subjected to qPCR to determine *ITGA4*, *ITGB1* and *CXCR4* expression (n=4-6; $^{\Delta\Delta\Delta}p<0.001$, $^{\Delta\Delta}p<0.01$ and $^{\Delta}p<0.05$). (E) Cells were exposed to cycloheximide (CHX; 100 μg/ml) for the indicated times and then tested by immunoblotting.

Figure 4. Bortezomib-resistant RPMI-8226 cells show higher *in vitro* and *in vivo* α4β1 function than parental cells. (A) Cells were subjected to adhesion assays to the indicated α4β1 ligands coimmobilized with CXCL12 (n=3; $^{\Delta}p<0.05$). (B, left) Parental and BTZ-resistant

RPMI-8226 cells were intravenously inoculated into NSG mice, which were treated every 2 days with control or anti-α4 antibodies. Data represent percentages of myeloma cell infiltration in the BM as assessed by HLA^+ human expression using flow cytometry. (Right) The expression of α4 on the BM infiltrated MM cells was analyzed by flow cytometry (n=7-9 bone marrow analyses). Bone marrow infiltration was significantly increased, $^{\Delta\Delta\Delta}p<0.001$, or decreased, $^{***}p<0.001$. (C) Myeloma cell infiltration in the BM of NSG mice was determined by RT-qPCR measuring the ratio of human *GAPDH* versus mouse *Tbp* expression (n=7-8; $^{\Delta\Delta\Delta}p<0.001$).

Figure 5. Role of NF-κB in upregulated α4β1 expression and function on BTZ-resistant MM cells. (A) Cells incubated without (-) or with BTZ (20 nM, 48 h) were analyzed by immunoblotting to test for expression of the indicated proteins. (B) Cells were analyzed by RT-qPCR for expression of the NF-κB targets *BIRC5* and *HIF1A* (n=3; $^{\Delta\Delta}p<0.01$, $^{\Delta\Delta\Delta}p<0.001$). (C) Cells were incubated for 24 h in the absence or presence of BAY-11-7082 (10 μM), and expression of *ITGA4*, *ITGB1* and *BIRC5* was determined by RT-qPCR (n=2; $^{***}p<0.001$, $^{*}p<0.05$). (D) Cells were nucleofected with the indicated siRNA, and expression of *NF-κB1* (left) and *ITGA4* (right) was tested by RT-qPCR (n=2-3; $^{**}p<0.01$, $^{*}p<0.05$). (E, left) siRNA-silenced cells were subjected to flow cytometry for detection of cell membrane α4 expression. Data show fold induction of fluorescence intensity values referred to control siRNA transfectants that were given a value of 100 (n=5; $^{***}p<0.001$). (Right) Transfectants were subjected to adhesion assays to CS-1/FN (n=3; $^{*}p<0.05$).

Figure 6. Prognostic value of *ITGB1* expression in MM. Correlation between the levels of *ITGB1* expression at diagnosis and progression-free survival (A), and overall survival (B) of BTZ/IMIDs-treated patients in the MMRF CoMMpass Study dataset. Kaplan–Meier curves represent a bi-level state expression (high and low) of *ITGB1*. (C, D) Multivariate analysis of synergy between *ITGB1* and high-risk genetic factors displaying Progression-Free Survival (C) and Overall Survival results (D). Kaplan–Meier curves showing the combined study of Amp1q and expression levels of *ITGB1* for Progression-Free Survival (E), and Overall Survival (F) of MM patients from the CoMMpass Study. (Low=Low expression of the *ITGB1*; High=High expression of the *ITGB1*).

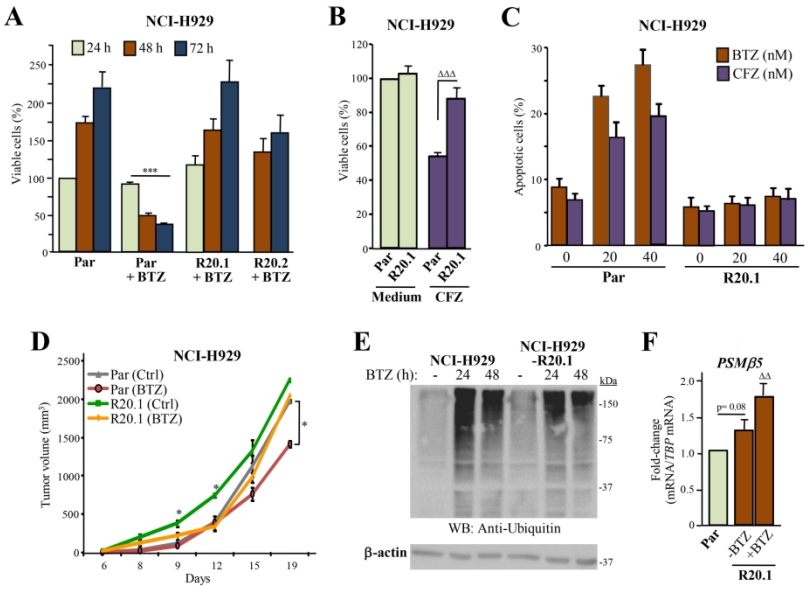

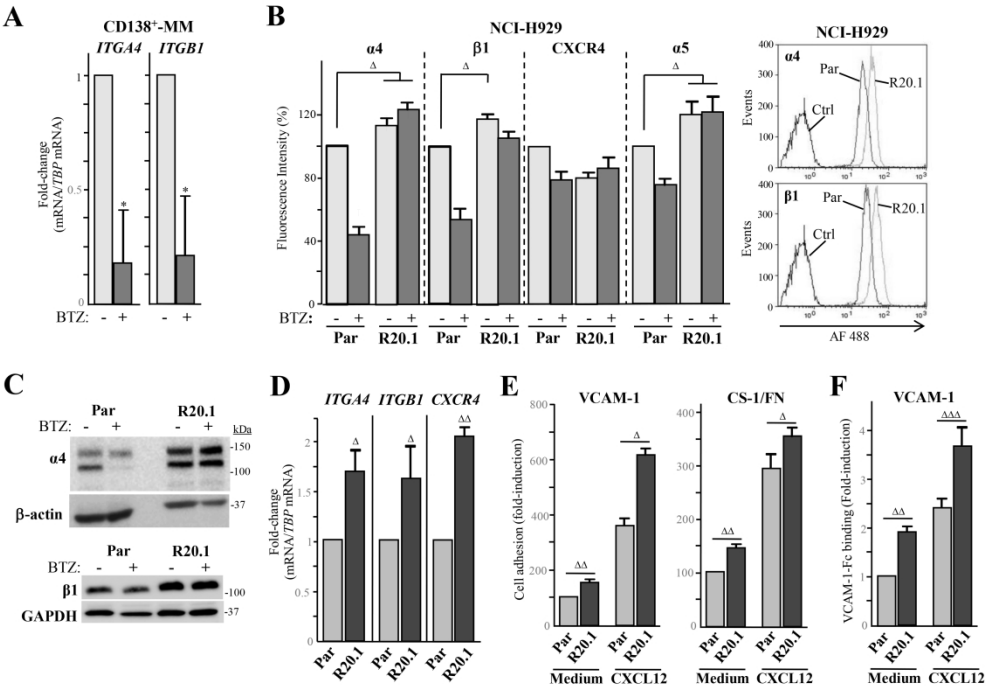

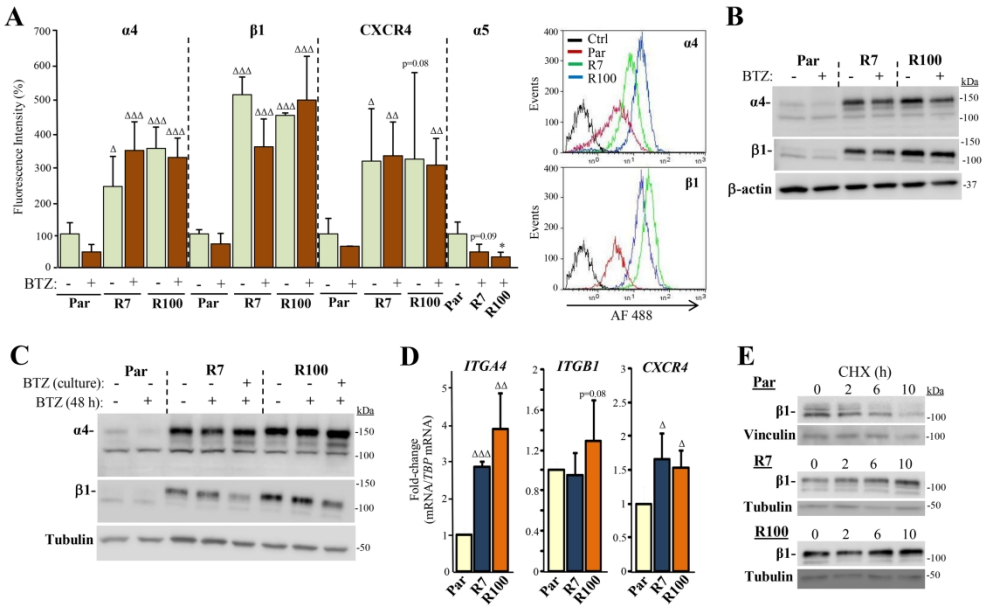

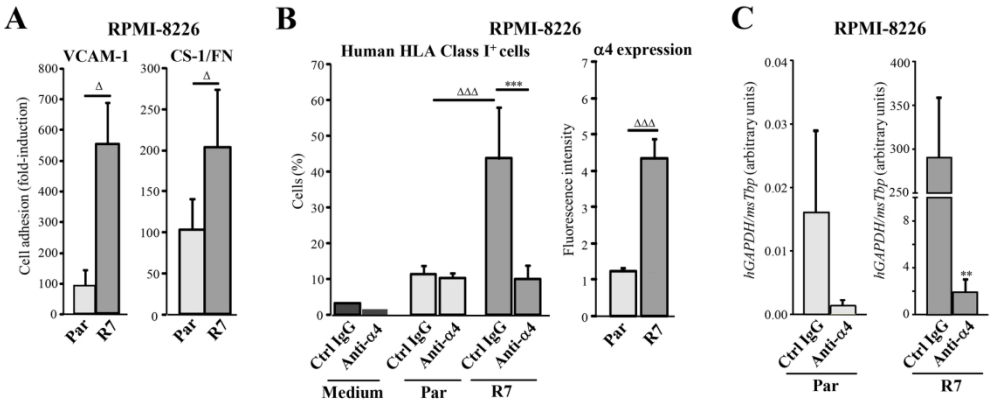

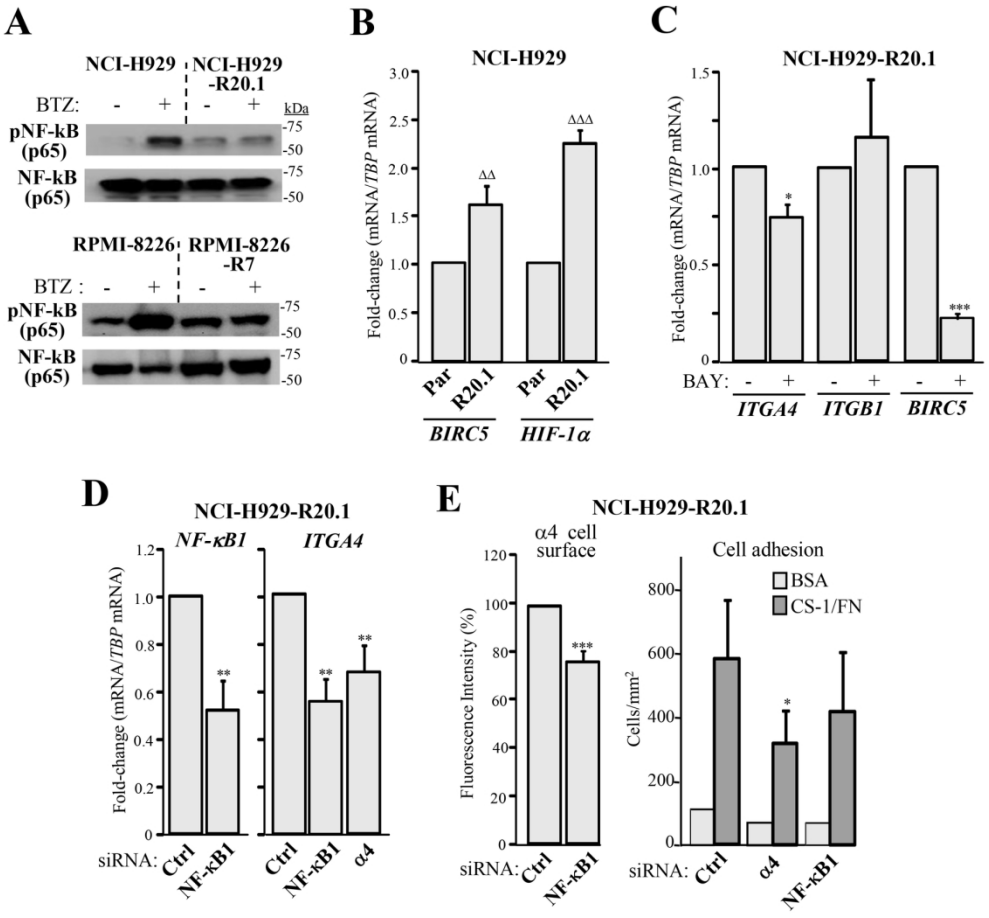

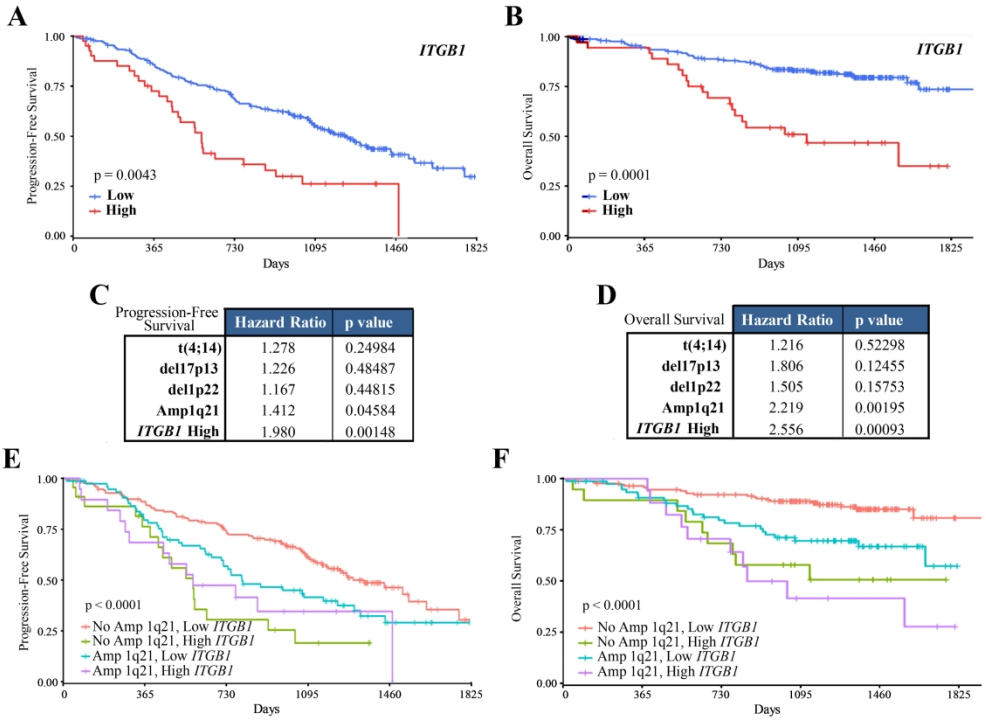

C

Progression-Free Survival	Hazard Ratio	p value
t(4;14)	1.278	0.24984
del17p13	1.226	0.48487
del1p22	1.167	0.44815
Amp1q21	1.412	0.04584
***ITGB1* High**	1.980	0.00148

D

Overall Survival	Hazard Ratio	p value
t(4;14)	1.216	0.52298
del17p13	1.806	0.12455
del1p22	1.505	0.15753
Amp1q21	2.219	0.00195
***ITGB1* High**	2.556	0.00093